

CHRISTOPHE L. HÉBETTE^{1),2)}, JAN A. DELCOUR²⁾, MICHEL H. J. KOCH¹⁾,
KARL BOOTEN³⁾, HARRY L. REYNAERS^{1),*)}

Crystallization and melting of inulin crystals. A small angle X-ray scattering approach (SAXS)

Summary — Bulk crystallization of the biopolymer inulin from concentrated solutions results in the same macroscopic and microscopic morphologies as those found for synthetic polymers. Optical and electron microscopy confirm the lamellar nature of the crystals and their arrangement into stacks of lamellar crystals in superstructures like axialites and spherulites. There is evidence for the occurrence of folded chain lamellar crystals. These findings justify the attempt to explore the crystallization and melting of inulin by investigating the morphology of inulin crystals by time-resolved small angle X-ray scattering. The thickness of the lamellar crystals observed by SAXS varies with the degree of supercooling — dynamically or isothermally — as observed for synthetic polymers crystallized from the solution. The complex melting behaviour of polydisperse inulin, crystallized from the concentrated solution, as observed by DSC, and previously describe by the present authors, can be explained by the occurrence of thin lamellae with lower thermal stability (endotherms I and II) together with thicker lamellae composed of the longer chains with a higher melting temperature (endotherms III and IV), the latter lamellae being able to thicken upon annealing by recrystallization or solid state reorganisation. The broad range of molar masses proper to the samples, the different crystallization conditions (temperature, isothermal and dynamic cooling and melting) account for fractionation and the presence of partially overlapping populations of lamellar stacks with different l_c 's and hence different thermal stabilities. The reported experiments are a basis for the exploration of the semi crystalline nature of inulin gels.

Keywords: inulin, biopolymers, SAXS, crystallization, melting.

KRYSTALIZACJA I TOPNIENIE INULINY BADANE TECHNIKĄ MAŁOKĄTOWEGO ROZ-
PRASZANIA PROMIENIOWANIA RENTGENOWSKIEGO (SAXS)

Streszczenie — Krystalizowany ze stężonych roztworów biopolimer inulinowy [wzór (I)] wykazuje makro- i mikromorfologię analogiczną do morfologii krystalicznych polimerów syntetycznych, krystalizowanych w podobnych warunkach. Płytkowy charakter kryształów inuliny potwierdza zarówno mikroskopia optyczna (rys. 3, 4), jak i elektronowa (rys. 5). Kryształy te zwane lamelami krystalicznymi tworzą, tzw. stosy lamelarne (rys. 6), a te z kolei kuliste agregaty – sferolity bądź aksjality. Morfologię kryształów inuliny badano metodą SAXS (rys. 7, 8), stwierdzając, że grubość płytek zależy od warunków krystalizacji (chłodzenia i topnienia izotermicznego bądź dynamicznego). Na podstawie krzywych topnienia skryształizowanej ze stężonego roztworu polidispersyjnej inuliny, można wyjaśnić występowanie cienkich płytek krystalicznych o mniejszej stabilności termicznej (endotermy I i II) wraz z grubszymi lamelami, złożonymi z dłuższych łańcuchów, o wyższej temperaturze topnienia (endotermy III i IV). Te ostatnie wykazują tendencję do zagęszczania (tworzenia agregatów) w procesie rekryształizacji lub w wyniku reorganizacji struktury łańcuchów stałej inuliny. W szerokim zakresie mas molowych, właściwych dla badanych próbek, i w różnych warunkach krystalizacji obserwujemy frakcjonowanie i częściowe pokrywanie się stosów lamelarnych krystalitów z różną wartością l_c (średniej lamelarnej grubości) i różną stabilnością cieplną. Przedstawione wyniki są podstawą do stwierdzenia semikrystalicznej struktury żeli inuliny.

Słowa kluczowe: inulina, biopolimery, SAXS, krystalizacja, topnienie.

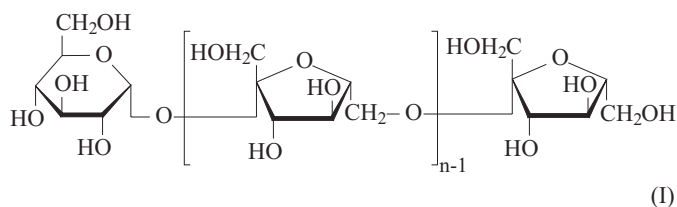
¹⁾ Catholic University of Leuven, Department of Chemistry, Section Molecular and Nanomaterials, Celestijnenlaan 200F B-3001 Leuven-Heverlee Belgium.

²⁾ Leuven Food Science and Nutrition Research Centre, Catholic University of Leuven, Kasteelpark Arenberg 20-bus 2463 B-3001 Leuven-Heverlee Belgium.

³⁾ ORAFIT, Aandorenstraat 1, B-3300 Tienen Belgium.

*) Author of correspondence; e-mail: harry.reynaers@chem.kuleuven.be

Inulin is a linear fructan consisting of β -2,1-linked D-fructofuranose units and one terminal α -1,2-linked D-glucopyranose unit [Formula (I)]. The polydispersity of the molecular chain length depends on the plant species (*e.g.* *Cichorium intybus* L. and *Dahlia* L.) and variety, the plants' life cycle and the weather conditions



during its growth and harvest [1–10]. Inulin containing plants are *e.g.* chicory (*Cichorium intybus* L.), Jerusalem artichoke, dahlia flowers, onions [1–9]. Inulin, the number two storage polysaccharide after starch, has only recently received considerable interest. The growing consumption of inulin over the past 20 years is the result of its combination of a low calory soluble dietary fiber and fat mimetic properties. Inulin is also currently under investigation as a packaging material for targeted drug delivery in the human colon [10]. Other non-food applications of inulin derivatives are in the oil industry, paper and pulp industry, water treatment and detergents. In order to meet the growing demand for inulin, stimulated by the increasing number of food and non-food applications, the current industrial process for the extracting of inulin involving polymer crystallization needs to be optimized. The crystallization of synthetic polymers from the melt and from dilute solutions into stacks of lamellar crystals and extended chain lamellar crystals has been extensively described in literature [11–16]. The aim of the present paper is to provide a more fundamental understanding of the crystallization and melting of inulin from concentrated solutions, obtained after hot water extraction of sliced chicory roots. Indirect evidence was obtained by differential scanning calorimetry [17]. Typical DSC traces exhibit three or four partially overlapping melting endotherms that vary as a function of cooling rate during crystallization and storage time at 25 °C of the crystalline suspensions. The formation and morphology of these inulin crystals has not yet been studied for concentrated inulin solutions although these are the two main keys to a more efficient isolation process.

Moreover, one of the characteristics of the semicrystalline inulin powders is that they form gels when intensively blended with water. The results of the present research are mainly based on experiments involving time-resolved synchrotron radiation, small angle X-ray scattering (SAXS) and optical and electron microscopy in order to characterize crystallization, crystallinity and crystal morphology of inulin under processing conditions.

EXPERIMENTAL

Materials

Inulin powders used for the present study are either a commercial grade inulin called RAFTILINE[®] ST or RAFTILINE HP, both kindly provided by ORAFIT, Tiense Suikerraffinaderij N.V., Tienen, Belgium [18]. The polydispersity of the inulin changes slightly with the time and year of harvest [19–21], but most powders used here have a comparable polydispersity ($DP_{min} = 1$, $DP_{max} = 85$, $DP_n = 12$ and $DP_w = 17$). Here DP_w and DP_n stand for the weight average and number average degree of polymerization together with the minimum DP_{min} and maximum number DP_{max} of fructose units in a chain as obtained by DIONEX-High Performance Anion Exchange Chromatography. Preparative gel filtration of a 10 wt. % Raftiline HP batch was used to obtain one sample with a more narrow chain length distribution, $DP_{min} = 39$ and $DP_{max} = 85$ [22].

Methods of investigations

- Optical microscopy (OM) was carried out using an Olympus BH-2 polarization microscope at 500 times magnification.
- Electron microscopy (TEM) experiments were done using a Philips Transmission Electron Microscope.
- Turbidimetry.

A sealed glass tube (length 150 mm, radius 7.5 mm, thickness 1 mm) containing the sample was placed in a glass container heated with a temperature controlled oil bath. A thermocouple was placed in the stirred sample to monitor its temperature. The glass tube was positioned in a laser beam generated by a Spectra Physics Model 133 laser and the transmitted beam intensity was continuously monitored by a photocell. This setup allowed continuous monitoring of the transmitted beam intensity at $2\theta = 0^\circ$ as a function of time and hence temperature. The onset of turbidity corresponded approximately to 1 % difference in the transmitted beam intensity between the solution and the fully crystallized sample.

– Time-resolved synchrotron radiation WAXS and SAXS patterns were recorded on the X33 double focussing monochromator-mirror camera of the EMBL-outstation at the storage ring DORIS III of the Deutsches Elektronen Synchrotron (DESY) in Hamburg, using the standard data acquisition system [23]. All data processing of the SAXS patterns was handled by the OTOKO software package [24]. The data are normalised to the incident beam intensity and corrected for the detector response. The crystal suspension consists of three phases: the solvent, the crystalline lamellae and the amorphous material between the lamellae. By subtracting the solvent scattering from the total scattering one obtains the scattering from the amorphous and crystalline phase. The channel numbers of the detector are converted into the values of the modulus of the

scattering vector $s = 2 \sin \theta / \lambda$, where 2θ is the scattering angle and λ is the wavelength of the incident X-ray beam (0.15 nm), by using the small angle reflections of a dry rat tail collagen sample ($d = 64.5$ nm) as the standard. Subsequently the linear correlation function $CF(x)$ [equation (1)] is calculated in this work following procedures fully described in [25] with references to the original contributions by Vonk [26] and Strobl [27].

$$CF(x) = \int s^2 I(s) \cos(2\pi xs) ds \quad (1)$$

It is interesting to note that only recently such a very flexible software package became available to facilitate and to speed up SAXS data analysis for two phase systems [28].

Accepting a linear two-phase stack-type model of lamellar crystals for inulin, two parameters [the long period L_p and the position A of the first intersection of $CF(x)$ with the abscissa] are extracted from the correlation function (Fig. 1). Since $A/L_p = \phi(1 - \phi)$, with ϕ and $(1 - \phi)$ respectively the volume fractions of the crystalline and intralamellar phases within the lamellar stack, two solutions

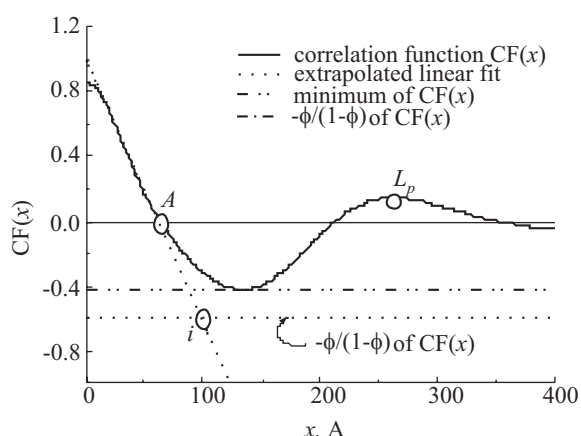


Fig. 1. A correlation function $CF(x)$ as a function of length x [Å] (after [25])

for ϕ are obtained. With this information the average lamellar thickness l_c and the average amorphous intralamellar space l_a are calculated from the formulae

$$l_c = L_p \cdot \phi \text{ and } l_a = L_p - l_c$$

Another important parameter is the invariant Q [equation (2)] which is a measure of the scattering power of the system:

$$Q = 4\pi \int s^2 I(s) ds = K \alpha_s (\rho_c - \rho_a)^2 \phi(1 - \phi) \quad (2)$$

where: ρ_c — the electron density of the lamellar crystals, ρ_a — the electron density of the amorphous material between adjacent lamellae, α_s — the volume fraction of the lamellar crystals in the irradiated sample volume, K — a constant depending on the experimental conditions.

As equation (2) shows, Q can be determined by integrating a plot of $I(s)s^2$ as a function of s . If we consider the square of the density difference between the crystalline and

amorphous phase to be constant, the ratio of Q over $\phi(1 - \phi)$ gives the evolution of α_s times K . The factor $\alpha_s K$ decreases upon melting, except in case of recrystallization where it decreases less or even increases upon heating. The invariant is a very sensitive parameter to assess crystallization, fractionated crystallization, melting and recrystallization in two phase systems, as illustrated below.

RESULTS AND DISCUSSION

The molecule of inulin can be described as a polyoxyethylene main chain to which the fructose moieties are attached without being a part of the molecular backbone. Hence inulin has an unusually high conformational flexibility for a polysaccharide. André *et al.* [29] as well as Marchessault *et al.* [30] reported that crystallization from very diluted solutions results in thin but laterally extended — between 1–2 μm in diameter — lamellar crystals, as is generally the case for ‘synthetic’ polymers crystallized from very dilute polymer solutions. However the thickness of the crystals perpendicular to the lamellar plane was not reported. Such crystals were used by these authors to determine the single crystal structure of inulin at the level of the unit cell. From the most recent analysis of André *et al.* [31] two crystal structures emerge both involving the inulin chains in a six-fold helical conformation. The first one, a monohydrated polymorph with an orthorhombic $P2_12_12_1$ space group has cell parameters $a = 1.67$ nm, $b = 0.98$ nm, $c = 1.47$ nm, with six fructose units per helical repeat resulting in a length of 0.245 nm per fructose unit. The second one, a semi-hydrated polymorphic orthorhombic structure with space group $P2_12_12_1$ has dimensions $a = 1.67$ nm, $b = 0.965$ nm and $c = 1.44$ nm. Comparison of the positions and the relative intensities of the powder diffraction maxima of our semi crystalline inulin samples, obtained using a wide-angle X-ray powder diffractometer, reveals that all our samples consist of the hydrated inulin crystal polymorph combined with an amorphous fraction. Crystallization from highly concentrated solutions is very different from that in the very diluted regime. Here we present the crystalline morphology of inulin crystallized from highly concentrated solution as studied by OM, TEM and SAXS.

Bulk inulin crystallization from concentrated solutions

When transparent concentrated inulin solutions are cooled down from 96 °C to 25 °C a white dispersion of inulin crystals forms in the aqueous inulin-water solution. The onset of turbidity can be determined visually or by turbidimetry for different inulin concentrations and different cooling profiles. In this case, two types of cooling profiles were used: a dynamic cooling profile in which the 96 °C solution is cooled at 1 °C/min to 25 °C (a) and one involving cooling at 0.25 °C/min from 96 °C to 25 °C (b) and a heating run, on the sample with the cool-

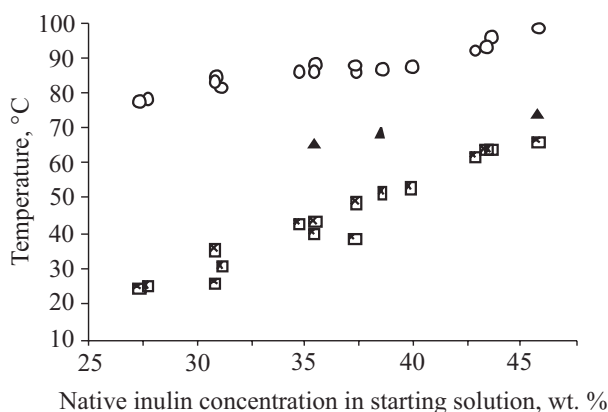


Fig. 2. A pseudo-phase diagram of native inulin: \boxtimes — first cloud point upon cooling at 1 °C/min from 96 °C to 25 °C, \circ — point at which a clear solution is reached upon heating at 1 °C/min from 25 °C, \blacktriangle — first cloud point upon cooling at 0.25 °C/min from 96 °C to 25 °C

ing conditions (a), at 1 °C/min from 25 °C to the temperature where a clear solution is again obtained. The onset of nucleation is detected by the formation of crystals large enough to scatter visible light, which occurs shortly after the first nucleation on the molecular scale. Nevertheless, the measured onset occurs sufficiently early in the crystallization to be used to construct a pseudo phase diagram (Fig. 2) giving the different temperatures and thus also times at which the onset of turbidity was measured for concentrated native inulin solutions (25–45 wt. %).

As expected, the lower cooling rate results in a slower crystallization but at higher temperature than that of the samples cooled at a higher rate. The melting temperature, which theoretically for equilibrium melting equals the highest possible isothermal crystallization temperature, is far above the onset obtained by dynamic cooling. The onset of nucleation for inulin thus is both time and temperature dependent completely in line with classical crystallization of synthetic polymers involving temperature dependent nucleation.

Crystalline morphology as observed by OM and TEM

The crystalline morphology of inulin is studied by optical microscopy. A wide variety of crystallite morphologies is found for the native inulin samples: at higher crystallization temperatures (e.g. 65 to 75 °C), needle-like axialites are formed. When the samples are dynamically cooled (e.g. 30–45 wt. % native inulin) from 96 to 25 °C at 1 °C/min at first some 8-like shaped crystallites are formed (Fig. 3) that develop into twinned or single spherulites (20–100 μm) with time (Fig. 4).

Apart from the wide variety of crystallite morphologies, the observation of several nucleations at different times during crystallization is characteristic for inulin. When cooling a solution of polydisperse inulin to room temperature, at higher temperatures, a limited number of crystallites is formed that grow into large spherulites.

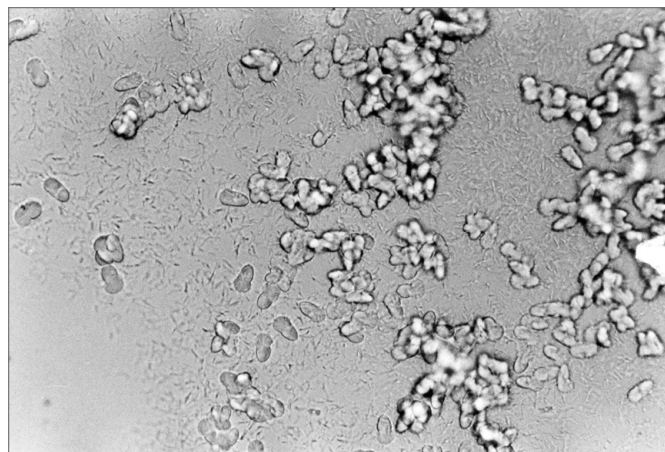


Fig. 3. Optical micrograph (500 \times) showing larger 8-like shaped and small needle-like crystals formed during the second nucleation of a 35 wt. % native inulin solution cooled from 96 °C to 25 °C at 1 °C/min and subsequently stored at 25 °C

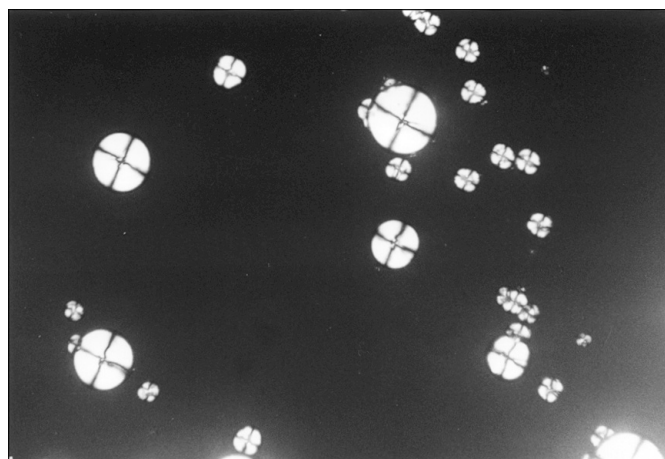


Fig. 4. Optical micrograph (500 \times) with crossed polarisers showing inulin spherulites with a Maltese cross, crystallized from a 30 wt. % native inulin solution at 25 °C, before the start of the secondary nucleation

Subsequent cooling to room temperature induces a second nucleation throughout the sample and gives rise to a very large number of 8-like shaped crystallites (0.1–10 μm). Transmission electron microscopy of an untreated cryosectioned inulin sample revealed a particle consisting of a network of radially oriented lamellae.

Stacks of lamellae are clearly visible (Fig. 5). Unfortunately the mean lamellar thickness cannot be estimated from the micrographs since the tilt of the lamellae relative to the direction of observation is unknown. However from the results above it can be concluded that the crystals obtained from concentrated solutions have a lamellar character which justifies a quantitative analysis of SAXS data in terms of the classical two phase model consisting of stacks of lamellar crystals separated by amorphous regions (Fig. 6).

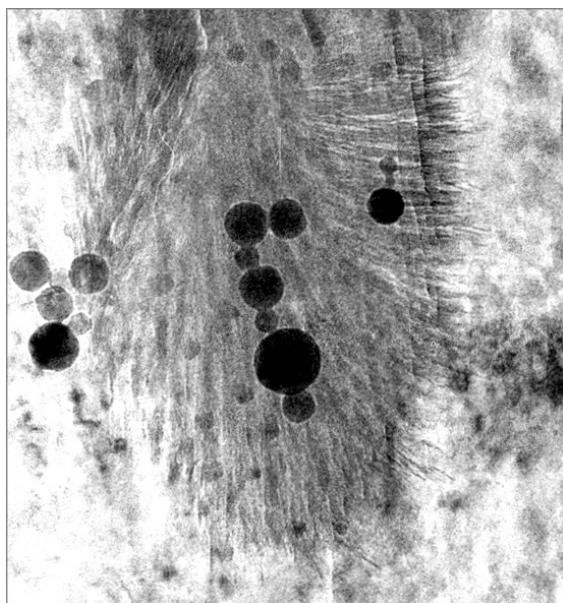


Fig. 5. TEM image of a cryosectioned 10 wt. % fractionated high MW inulin sample, isothermally crystallized at 25 °C. The lamellar superstructure of the crystallites is typical for semicrystalline polymers. The black circles on the picture are artefacts due to the formation of ice onto the sample

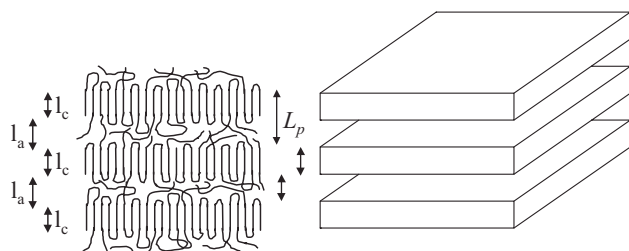


Fig. 6. The left diagram represents the front view of polymer chains associated with three lamellar crystals stacked on top of each other. Notice the backfolding of some chains, as well as the interconnection of the lamellae by some chains. The right drawing shows a 3-dimensional view of an idealised lamellar stack. The lamellar thickness l_c , the thickness of the amorphous layer in between the lamellae, l_a and the long period L_p , corresponding to the sum of l_a and l_c are indicated

Superstructure characterisation by small angle X-ray scattering: The evolution of the crystal thickness l_c as a function of different crystallization procedures

Figures 7a, b and c illustrate the evolution of l_c , l_w , L_p and Q for three differently crystallized 45 wt. % native inulin samples. For an isothermal crystallization (Fig. 7a) at 25 °C after quenching from 96 °C the situation is simple: l_c remains constant around the mean value of 28 Å since all chain lengths crystallize at a constant degree of supercooling.

This does not necessarily mean that the longer chains crystallize into lamellae of the same thickness as the shorter chains, since the former are less soluble, have a

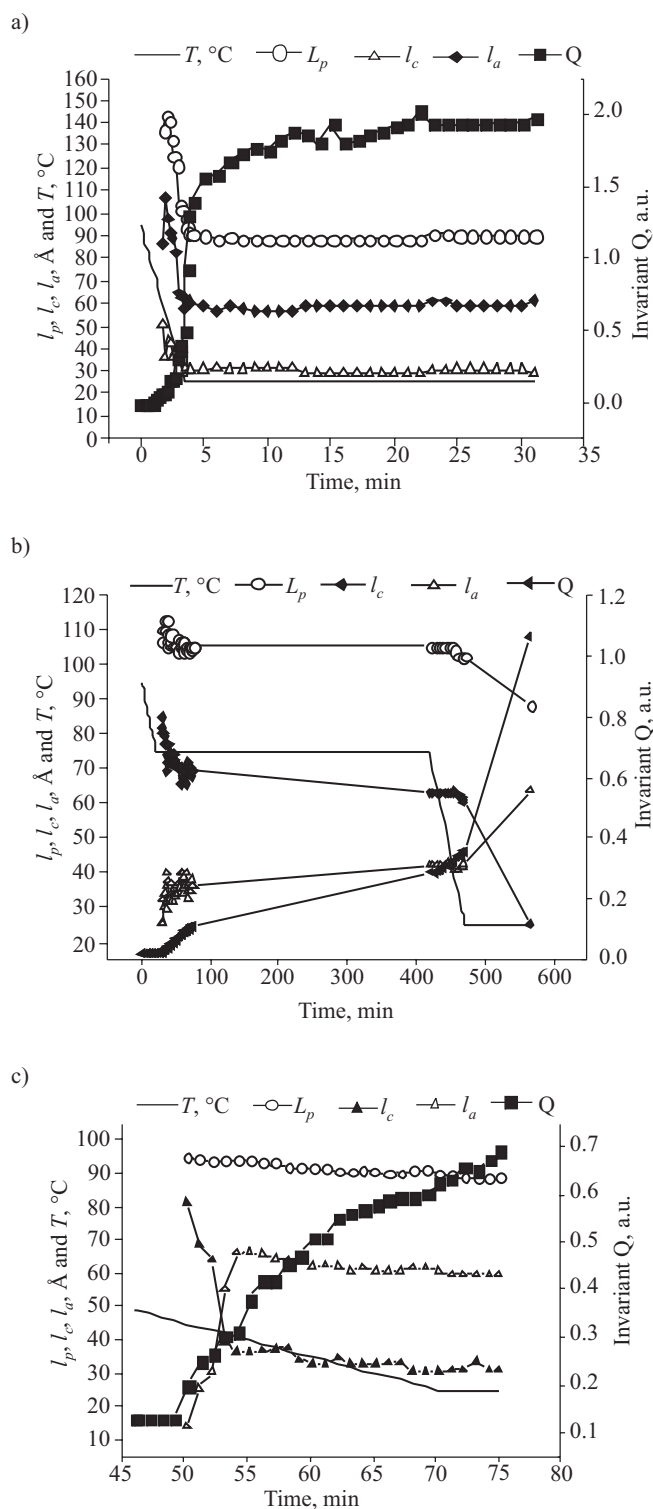


Fig. 7. Evolution of l_c , l_w , L_p and Q , as derived from time-resolved SAXS-measurements during crystallization, in a 45 wt. % native inulin sample crystallized under different conditions, namely: a — quenched from 96 °C to 25 °C and then isothermally crystallized at 25 °C, b — cooled from 96 °C to 75 °C at 1 °C/min, then isothermally crystallized at 75 °C, and subsequently cooled down to and stored at 25 °C, c — cooled from 96 °C to 25 °C at 1 °C/min and then stored at 25 °C

higher equilibrium melting temperature (T_m^0) and thus higher degree of supercooling than for the shorter chains,

yielding a smaller thickness. The polydispersity of inulin results in the formation of a distribution of lamellar thicknesses. For isothermal crystallization at 75 °C (Fig. 7b), cooling from 96 °C to 75 °C at 1 °C/min, and subsequently cooling to and storage at 25 °C, a small decrease of l_c from 85 Å to 63 Å is observed as a function of isothermal residence time, followed by a steep decrease of l_c to 25 Å upon cooling and storage at room temperature.

This particular crystallization behaviour, called temperature-dependent fractionated crystallization, implies that the longer inulin chains crystallize at higher temperatures into thicker inulin crystals, while the intermediate and shorter inulin chains, still fully dissolved at these higher temperatures, only crystallize upon further cooling to the room temperature. The small decrease in l_c during the isothermal crystallization period at 75 °C is attributed to the different crystallization kinetics of the crystallizing chains. At 75 °C, only inulin chains above a certain MW meet the supersaturation conditions for crystallization from solution. In this polydisperse group of chains, the solubility decreases while the supersaturation increases with the MW. Therefore the longer chains crystallize both faster and at higher temperature, giving thicker lamellae, whereas the slightly shorter chains crystallize both more slowly and at lower temperature, giving slightly thinner lamellae. Of course, both crystallizations overlap in time and part of the chains crystallize at the same temperature into the same lamellae or at least in lamellae of nearly equal thickness. The steep decrease from 63 to 25 Å upon cooling and storing at 25 °C is attributed to the overall crystallization into thin lamellae of the intermediate and low MW inulin. Such temperature fractionated crystallization is typical for polymeric materials. When cooling the 45 wt. % solution at 1 °C/min (Fig. 7c), the evolution of l_c is in between the two previous crystallization processes.

At high temperature part of the high MW inulin crystallizes, but during dynamic cooling time is too short for all chains of a given molar mass to crystallize. As the longer chains continue crystallizing and the solution is cooled below a certain temperature, also the intermediate and shorter chains progressively start crystallizing into thinner lamellae. From these and other observations below one can conclude that several populations of lamellar crystals of different thickness are formed during crystallization, due to the presence of chains of different molar masses having different degrees of supersaturation at identical crystallization temperatures. The changes in the invariant make clear that Q is indeed a very sensitive tool to assess changes in crystallinity. As stated above, Q is proportional to the product $\phi(1 - \phi)$ which displays a parabolic evolution as a function of ϕ . Consequently the onset and changes in degree of crystallinity can easily be detected for values in the regions $0 < \phi < 35$ and $65 < \phi < 100$. Clearly, the invariant is less sensitive for the intermediate values of the crystallinity, i.e. $35 < \phi < 65$. As $\phi(1 - \phi)$ has the maximum value for $\phi = 0.5$, the invariant of sam-

ples with $\phi < 0.5$ first increases upon crystallization up to 0.5 and then decreases at higher crystallinities.

Structural changes upon heating and melting

The evolution of l_c , l_w , L_p , $\phi(1 - \phi)$, $\alpha_s K$ and Q of a 20 wt. % DP 39–85 sample are plotted for a heating run from 25 °C to 95 °C at 1 °C/min (Fig. 8). Between 25 °C and 58 °C L_p and l_c evolve similarly, from 59 °C to 70 °C the increase of l_c is clearly larger than that of L_p upon further melting.

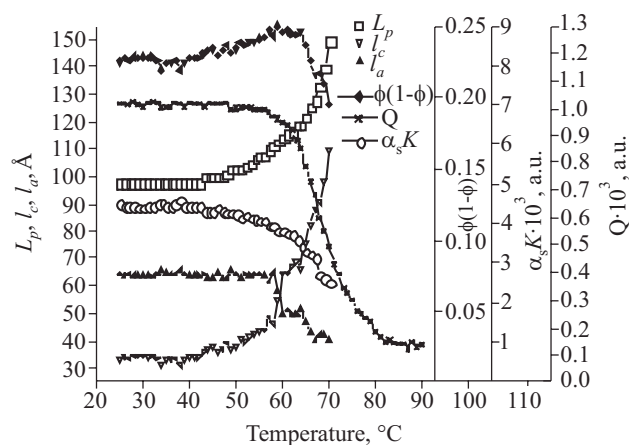


Fig. 8. Evolution of l_c , l_w , L_p , $\phi(1 - \phi)$, $\alpha_s K$ and Q of the 20 wt. % DP 39–85 sample heated from 25 °C to 95 °C at 1 °C/min, as derived from time-resolved SAXS-measurements

The increase in l_c between 25 °C and 58 °C coincides with a slight decrease of $\alpha_s K$, suggesting that only a very small volume fraction of the lamellae in the irradiated volume has molten. Above 62 °C the drop in $\alpha_s K$ indicates extensive melting, although at 70 °C more than 50 % of the original lamellar volume fraction is still present. The doubling of l_c from 33 Å at 25 °C to 66 Å between 60 °C and 65 °C, followed by an increase to 90 Å and then 110 Å, might indicate a recrystallization involving partial unfolding of the longest chains to allow thickening. The crystal structure reported by André *et al.* [31] suggests that an extended helix of DP 80 has a length of 196 Å. The inulin chain is very flexible and it can be shown using Stuart-Briegleb models that 6 monomer units are needed to realise adjacent reentry at the lamellar surface; this implies that the chain traverses a lamella of $l_c = 33$ Å about 5 times. Hence, as temperature rises, l_c increases and a smaller number of chains is sufficiently long to fit into the new lamellae, explaining the observed decrease in $\alpha_s K$. Moreover, the stepwise drop of l_a and the concomitant doubling of l_c also point towards recrystallization. Further evidence for recrystallization between 60 °C and 70 °C was found in our previous DSC study on a very polydisperse, 45 wt. % native inulin sample [17]. Above 70 °C, no clear side maximum could be detected in the correlation function, probably due to the transition from

stacks of lamellar crystals into individual lamellae, caused by recrystallization of the longest chains interconnecting the lamellae.

CONCLUSIONS

Crystallization of biopolymers from concentrated solutions remains poorly studied. The present experiments with two different MW inulin fractions, crystallized from concentrated solutions, clearly point to the occurrence of the same morphologies as found for synthetic polymers. Optical and electron microscopy confirm the lamellar nature of the crystals and their arrangement into stacks of lamellar crystals and superstructures with axialites and spherulites. There is clear evidence for folded chain lamellar crystals. These findings justify an attempt to explore the morphology of inulin crystals, as obtained under industrial processing conditions, by small angle X-ray scattering. The thickness of the lamellar crystals observed by SAXS varies with the degree of supercooling — dynamically or isothermally — as observed for synthetic polymers crystallized from solution or from the melt. The complex melting behaviour of polydisperse inulin, crystallized from concentrated solution, as observed by DSC, can be understood by the occurrence of thin lamellae with lower thermal stability (endotherms I and II) together with thicker lamellae, mostly composed of the longer chains and co-crystallized shorter chains, with a higher melting temperature (endotherms III and IV); the latter lamellae are able to thicken upon annealing by recrystallization or solid state reorganisation (as observed by SAXS and DSC). The broad range of molar masses proper to the samples, the different crystallization conditions (temperature, isothermal conditions or dynamic cooling) account for the presence of a large number of lamellar stacks with quite different l_c 's. Crystallization of inulin under industrial processing conditions clearly follows the trends observed for synthetic polymers which also makes SAXS an appropriate tool for studying crystallization and melting of inulin. New SAXS experiments will be needed to simulate the DSC conditions previously reported in order to adequately describe the complex melting of inulin.

REFERENCES

1. Timmermans J. W., Van Leeuwen M. B., Tournois H., de Wit D., Vliegthart J. F. G.: *Carbohydr. Chem.* 1994, **13**, 881.
2. Timmermans J. W.: "PhD-thesis", University of Utrecht, the Netherlands 1997.
3. Franks F.: "Polysaccharides In Food" (Eds. Blanshard J. M. V., Mitchell J. R.), 1st ed., Butterworths, London 1979, p. 33.
4. French A. D.: *Plantphysiol.* 1989, **134**, 125.
5. French A. D.: "Inulin and inulin containing crops" (Ed. Fuchs A.), 1st ed., Elsevier Plantscience, Amsterdam 1993, p. 121.
6. Robertfroid M., Gibson G. R., Delzenne N.: *Nutr. Rev.* 1993, **51**, 137.
7. De Leenheer L., Hoebregs H.: *Starch/Stärke* 1994, **46**, 193.
8. Van den Ende W.: "PhD-thesis 303", Faculty of Agricultural and Applied Biological Sciences, Catholic University of Leuven, Belgium 1996.
9. Van Loo J., Coussement P., De Leenheer L., Hoebregs H., Smits G.: *Crit. Rev. Food Sci. Nutr.* 1995, **35**, 52.
10. Vervoort L., Van den Mooter G., Augustijns P., Busson R., Toppet S., Kinget R.: *Pharm. Res.* 1997, **14**, 1730.
11. Morris E. R.: "Polysaccharides in Food" (Eds. Blanshard J. M. V., Mitchell J. R.), 1st ed., Butterworths, London 1979, p. 15.
12. "Polymer Physics" (Ed. Gedde U.), 2nd ed., Chapman & Hall, London 1995.
13. "Macromolecular Physics" (Ed. Wunderlich B.), Vol. 2 "Crystal Nucleation", Growth, Annealing, 1st ed., Academic Press, New York 1976, Ch. 5, p. 83.
14. Prasad A., Mandelkern L.: *Macromolecules* 1989, **22**, 91.
15. Sawodny M., Asbach G. I., Killian H. G.: *Polymer* 1990, **31**, 185.
16. Cohen Y., Cohen E.: *Macromolecules* 1995, **28**, 363.
17. Hébette C. L. M., Delcour J. A., Koch M. H. J., Booten K., Kleppinger R., Mischenko N., Reynaers H.: *Carbohydr. Res.* 1998, **310**, 6.
18. Tiense Suikerraffinaderij N. V., Orafti N. V.: Personal communications.
19. Vogel M.: "Inulin and inulin containing crops" (Ed. Fuchs A.), 1st ed., Elsevier Plantscience, Amsterdam 1993, p. 65.
20. Berghofer E., Cramer A., Schmidt U., Veigl M.: "Inulin and inulin containing crops" (Ed. Fuchs A.), 1st ed., Elsevier Plantscience, Amsterdam 1993, p. 77.
21. Huber A., Praznik W., Spies T., Kammerer S., Knabl C.: "Inulin and inulin containing crops" (Ed. Fuchs A.), 1st ed., Elsevier Plantscience, Amsterdam 1993, p. 231.
22. Hébette C. L. M.: "PhD-thesis 502", Faculty of Agricultural and Applied Biological Sciences, Catholic University of Leuven, Belgium 2002.
23. Boulin C. J., Kempf R., Gabriel A., Koch M. H. J.: *Nucl. Instrum. Methods Phys. Res. Sec. A* 1988, **269**, 312.
24. Boulin C. J., Kempf R., Koch M. H. J., Mc Laughlin S. M.: *Nucl. Instrum. Methods Phys. Res. Sec. A* 1986, **249**, 399.
25. Goderis B., Reynaers H., Koch M. H. J., Mathot V. B. F.: *J. Polym. Sci. Part B. Polym. Phys. Ed.* 1999, **37**, 1715.
26. Vonk C. G., Kortleve G.: *Kolloid Z. Z. Polym.* 1967, **220**, 19.
27. Strobl G. R., Schneider M.: *J. Polym. Sci. Polym. Phys. Ed.* 1982, **18**, 1343.
28. Rabiej S., Rabiej M.: VIII International Conference on X-Ray investigations of polymer structure, Wroclaw 2010, Book of Abstracts, p. 36.
29. André I., Putaux J. L., Chanzy H., Taravel F. R., Timmermans J. W., de Wit D.: *Int. J. Biol. Macromol.* 1996, **18**, 195.
30. Marchessault R. H., Bleha T., Deslandes Y., Revol J. F.: *Can. J. Chem.* 1980, **58**, 2415.
31. André I., Mazeau K., Tvaroska I., Putaux J.-L., Winter W. T., Taravel F. R., Chanzy H.: *Macromolecules* 1996, **29**, 4626.